Cell Mimics

International Edition: DOI: 10.1002/anie.201502920
German Edition: DOI: 10.1002/ange.201502920

Reversibly Triggered Protein–Ligand Assemblies in Giant Vesicles**

*Ruud J. R. W. Peters, Marlies Nijemeisland, and Jan C. M. van Hest**

Abstract: *External small-molecule triggers were used to reversibly control dynamic protein–ligand interactions in giant vesicles. An alcohol dehydrogenase was employed to increase or decrease the interior pH upon conversion of two different small-molecule substrates, thereby modulating the pH-sensitive interaction between a Ni-NTA ligand on the vesicle membrane and an oligohistidine-tagged protein in the lumen. By alternating the small-molecule substrates the interaction could be reversed.*

Compartmentalization is a key organizational feature in nature. It allows cells to spatially arrange enzymatic complexes in order for their processes to function more efficiently.[1] In eukaryotic cells, organelles are applied to spatially separate biosynthetic pathways.[2] Next to these permanent spatial assemblies of biomolecules, the cell also utilizes a host of dynamic interactions that temporarily interface proteins and ligands to control a cellular process. These dynamic assemblies often form and dissociate in response to changes in their interaction domains.[3] The cues can originate either from elsewhere inside the cell, or from the outer environment.

Cellular responses to external signals often involve signaling pathways facilitated by such a biomolecular assembly process, for example triggered by the binding of the signaling compound to a membrane-bound receptor or other protein and subsequently activating it. Many of these events involve protein–protein, or protein–ligand binding, which causes a change in protein or ligand localization and allows the cell to direct these molecules to the site of action.

Controlling and understanding these complex processes is of vital importance for unraveling the functioning of the cell. Research into protocells and artificial cell mimics has, among others, already focused on transcription and translation processes,[4] cytoskeletal structures,[5] the use of organelle subcompartments for spatial organization,[6] the induction of selective permeability,[7] and molecular crowding.[8] The dynamics of reversible protein–ligand interactions and assemblies inside cell mimics, however, has to our knowledge hardly been explored yet. These interactions, however, are of vital importance to the cell, as they contribute to cell signaling,[9] GPCR complex assembly,[10] improving cofactor regeneration systems and endocytosis-related processes.[11] Gaining spatiotemporal control over these processes can therefore aid in studying them in more detail,[12] but also in designing more complex cell-like systems that can respond to their environment.

To devise an artificial cell mimic of how cells can respond reversibly to external stimuli, that is, the addition of food sources, or signaling molecules, three elements should be combined: a cell-mimetic compartment, an externally triggered environmental change, and a reversible protein–ligand interaction. We use giant unilamellar vesicles (GUVs) as a cell-mimicking platform where the semipermeable nature of the lipid membrane allows small molecules to passively diffuse into the vesicle lumen and trigger a response inside. Through enzymatic conversion of the small molecule, a pH change can be induced[13] that allows for the selectively triggered assembly and disassembly of a protein–ligand complex. The pH change inside the GUVs can be controlled by using an alcohol dehydrogenase (ADH) that requires the natural cofactor NAD(H). During cofactor conversion protons are either consumed or produced, depending on the substrate used, as ADH is capable of both reducing ketones like acetone, and oxidizing alcohols like isopropyl alcohol (*i*PrOH) (Figure 1).

The maximum pH change is therefore also limited by the amount of cofactor present inside the system, and the directionality of the reaction can be reversed upon addition of the opposite trigger. The change in internal pH in the system can subsequently be used to promote a structural change by disturbing or forming a pH-sensitive protein–ligand interaction (Figure 1). A bright and acid-stable fluorescent protein called tdTomato[14] containing the commonly employed oligohistidine tag (His-tag) is used to bind a Nickel(II) nitrilotriacetic acid ligand (Ni-NTA)[15] on the GUV membrane in a pH-dependent and reversible manner.[16] Upon ADH-mediated acidification or neutralization of the GUV lumen, the interaction between the protein and membrane-bound ligand can be broken or formed, respectively. Here we aim to demonstrate with this system that external small-molecule stimuli can effect reversible structural changes inside giant vesicles (Figure 1 A,B).

As lipid membranes are only semi-permeable, first the permeability of the GUVs for the substrates was assessed. Giant vesicles were formed using the droplet transfer method[17] with a mixture of 1-palmitoyl-2-oleoyl-*sn*-glycero-3-phosphatidylcholine (POPC) and cholesterol (1:2 molar ratio). For protein binding the GUV membrane was supplemented with a Ni-NTA-presenting lipid (DGS-NTA-Ni) during vesicle formation. Confocal fluorescence microscopy and cryogenic scanning electron microscopy were used to

[*] R. J. R. W. Peters, M. Nijemeisland, Prof. J. C. M. van Hest
Bio-organic chemistry, Institute for Molecules and Materials, Radboud University Nijmegen
Heyendaalseweg 135, 6525 AJ, Nijmegen (The Netherlands)
E-mail: j.vanhest@science.ru.nl

[**] R.J.R.W.P. thanks the Dutch Science Foundation (NWO) for funding. J.C.M.v.H. acknowledges funding from the Dutch Ministry of Education, Culture and Science (Gravitation program 024.001.035).

Supporting information for this article is available on the WWW under http://dx.doi.org/10.1002/anie.201502920.

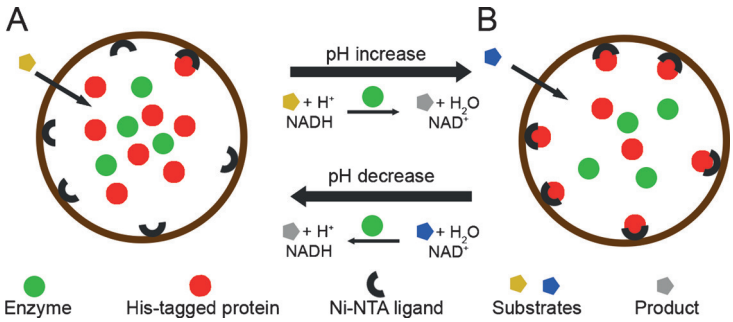

Figure 1. The localization and binding of a fluorescent His-tagged protein with a Ni-NTA-presenting lipid inside GUVs can be influenced by addition of an external substrate trigger. Upon addition of the trigger, ADH can be used to reversibly change the local pH inside the GUV to modulate the pH-sensitive interaction between Ni-NTA and the His-tagged protein. At acidic pH (A), the interaction is prevented, while upon increasing the pH, the interaction is induced (B) and vice versa.

verify the successful formation of GUVs (Figure S1 in the Supporting Information). Subsequently, ADH and the respective cofactor were loaded into GUVs. As NADH is fluorescent, its consumption or production by ADH was conveniently monitored by fluorescence microscopy upon external addition of the substrates acetone or *i*PrOH, respectively. For acetone, fluorescence decreased in GUVs due to NADH consumption (Figure S2B), while for *i*PrOH, evolution of NADH fluorescence was observed (Figure S2B). These results indicate that the GUVs are permeable to the small-molecule substrates, and they retain the larger enzymes and cofactors.

Next, the ability of the system to change and regulate the pH of the inner solution was explored. Bulk studies using a ratiometric pH-sensor were performed to follow pH changes caused by the enzymatic reaction. The sensor, containing carboxyfluorescein (Fluorescein) and tetramethylrhodamine (TAMRA), displays a pH-dependent increase in Fluorescein/TAMRA fluorescence emission ratio between pH 4.0 and 9.0 (Figure S3, depicted as horizontal calibration lines). A weak sodium phosphate buffer (0.5 mM) was applied to allow the enzymes to adjust the pH as the reaction progresses. Upon using 10 mM cofactor and 12 mM substrate, changes from pH 5.0 to over pH 7.0 and back were achieved (Figure S3). Notably, the reaction causing the pH decrease was considerably slower compared to the one responsible for the pH increase (Figure S3B). The diminishing reaction rate observed for the pH decreasing reaction corresponds to a pH-dependent decrease in ADH activity when using *i*PrOH as a substrate (Figure S3D), however, it eventually reaches pH 5.0, which is the expected disruption point for the Ni-NTA and His-tag complex. When using acetone, no notable change in ADH activity was observed between pH 5 and 7, which supports the fast pH increase caused by the addition of acetone (Figure S3A and S3D).

We then investigated the ability of the enzymes to generate and maintain the same pH change in GUVs using the pH sensor described above by confocal fluorescence microscopy. A pH increase was observed when triggering the GUVs with acetone (Figure 2A,C), while upon triggering with *i*PrOH the expected pH decrease was also achieved (Figure 2B,D). However, both actions required longer reaction times compared to the bulk experiments, likely due to the presence of the lipid membrane.

After having established the possibility to trigger a pH change in GUVs, we attempted to apply this to modulate protein assembly in the vesicles. To visualize this, fluorescent His_6-tagged tdTomato[14] (Figure S4) was encapsulated in GUVs with DGS-NTA-Ni lipid mixed in at different molar percentages during vesicle formation. To assess which conditions were required to achieve successful assembly and disassembly of tdTomato on the GUV membrane, amounts ranging from 0.1% up to 5% DGS-NTA-Ni were used in vesicles containing only the fluorescent

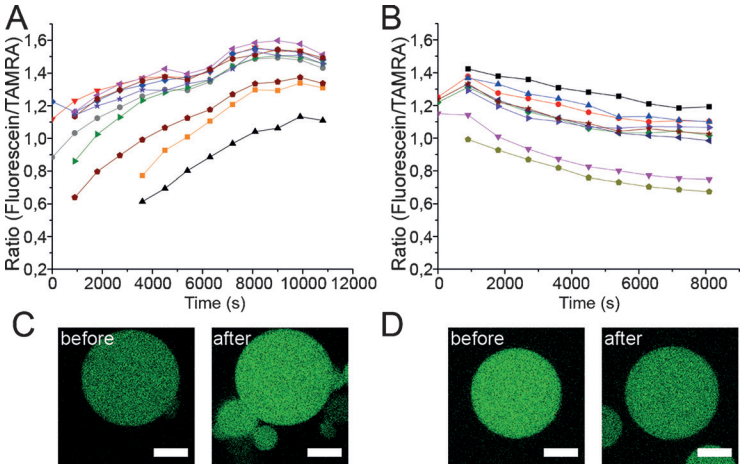

Figure 2. Confocal fluorescence microscopy experiments showing pH changes in individual GUVs as a result of the enzymatic reaction. Either a pH increase (A, C, with acetone) or decrease (B, D, with *i*PrOH) was induced. Changes in pH are visualized as a change in Fluorescein/TAMRA emission ratio, where a higher ratio represents a higher pH value. Scale bar is 10 μm.

protein, dissolved in either 10 mM NaH_2PO_4 buffer pH 7.0, to mimic assembly conditions, or pH 5.0 for disassembly. For 30 μm GUVs containing 0.5% DGS-NTA-Ni, it was calculated that a 1.1-fold excess of tdTomato (2.5 μM) was present inside the vesicle lumen. For all DGS-NTA-Ni concentrations membrane binding was observed at pH 7.0, except for 0.1% DGS-NTA-Ni (Figure S5B). At pH 5.0, only at 0.5% and 0.1% DGS-NTA-Ni membrane binding was inhibited (Figure S5A). This indicated that the ligand density was of vital importance to achieve reversible assembly in the pH range between 5.0 and 7.0, and that a ligand density that is too high could prevent disassembly of the complex. This is likely an effect of the multivalent nature of closely packed Ni-NTA ligands on the membrane.[15]

Using the system with 0.5% DGS-NTA-Ni lipid in the vesicle membrane and a starting pH of 4.8 or 7.0, the respective assembly and disassembly studies were performed. To monitor assembly, the ratio of lumen fluorescence intensity over membrane fluorescence intensity was mea-

sured. A ratio of 1 would therefore indicate uniform fluorescence in the GUV and complete disassembly, while a ratio close to 0 would indicate a high degree of membrane association for the protein. Both assembly and disassembly were observed upon addition of the respective triggers (Figure 3 and Figure S6), while no change in assembly was observed when ADH was not included in the GUVs, demonstrating the necessity of the pH change to trigger assembly (Figure S7). For membrane assembly, acetone was added, and a clear transition from a lumen/membrane ratio of 1.0 to ca. 0.3 was observed (Figure 3 A,B). This clearly demonstrated the small-molecule-triggered assembly of tdTomato on the GUV membrane. For GUVs where disassembly was triggered with *i*PrOH, however, dissociation appeared to be highly dependent on the starting pH in the system. Only the system with a starting pH of 6.1 showed complete disassembly in all vesicles (Figure 3 C,D). At pH 6.5 the response was slower and also not complete (Figure S6 A,B), while at pH 7.0, disassembly was even less pronounced (Figure S6 C,D). As the ensemble measurements previously showed that even from pH 7.0, a decrease to pH 5.0 could be achieved (Figure 2 B), the GUVs should be capable of reaching the point of disassembly. From our observations in GUVs, however, it appeared that the required pH was not reached when the reactions were started from a pH between 6.5 and 7.0. Therefore it might be possible that the GUVs were unable to build up and subsequently maintain the required pH gradient long enough for disassembly to occur. Generally, liposome-based pH gradients, displaying transmembrane pH differences which can be as high as 2–4 pH units,[18] are maintained by using solutions with a far higher buffering capacity compared to that of the system described here, and their dissipation due to leakage therefore takes a longer time. The durability of the ADH-based gradient not only depends on proton leakage and the weaker buffer, but also might be more limited due to a membrane plasticizing effect of the small molecule substrate, increasing the leakage rate. Also the amount of nicotinamide cofactor that is present, and the rate at which it can be converted in response to the changing pH in the GUV lumen might influence the stability of the gradient over time.

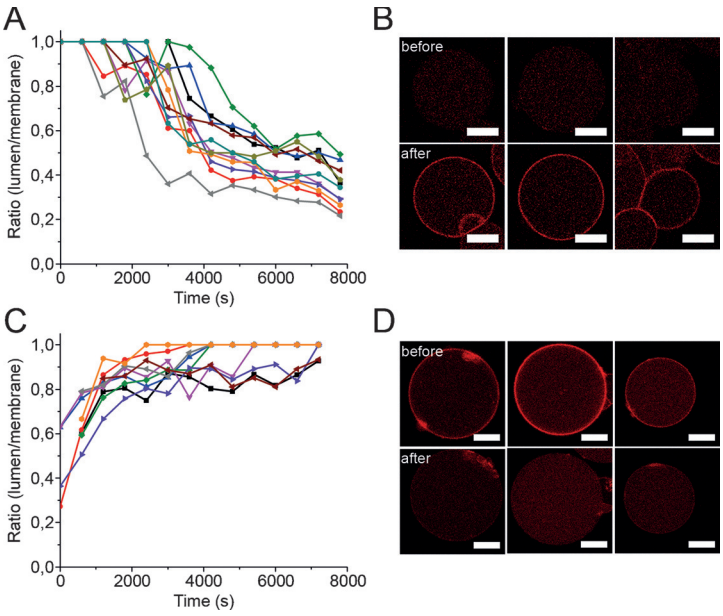

Figure 3. Assembly kinetics of His_6-tdTomato (2.5 μM) in 0.5% DGS-NTA-Ni GUVs upon acetone-induced pH increase starting from pH 4.8 (A) and disassembly kinetics upon *i*PrOH-induced pH decrease starting from pH 6.1 (C). Panels (B) and (D) display representative fluorescence images of GUVs before addition of the external trigger and after completion of the reaction. Assembly kinetics are expressed as the ratio of average lumen over average membrane fluorescence intensity and displayed from the moment GUVs settle into focus. Scale bar is 10 μm.

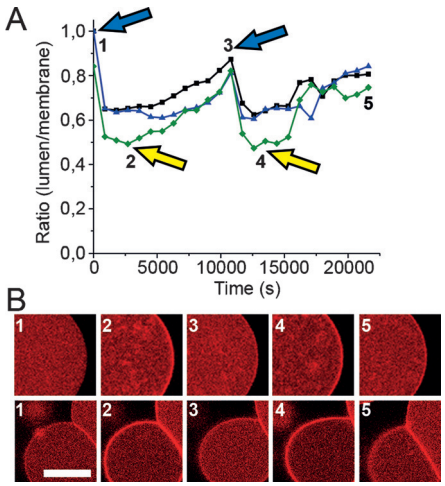

Figure 4. Reversible assembly and disassembly kinetics of tdTomato (2.5 μM) in individual surface-immobilized GUVs containing 0.5% DGS-NTA-Ni as a result of alternated addition of small molecule triggers. A) At $t = 0$ s (blue arrow), 20 mM acetone was added to the external solution, triggering assembly. At $t = 2700$ s (yellow arrow), acetone was replaced with 20 mM *i*PrOH to induce disassembly. At $t = 11\,700$ s (blue arrow), *i*PrOH was again replaced with acetone, while at $t = 13\,500$ s (yellow arrow), acetone was substituted by addition of *i*PrOH. B) Fluorescence microscopy images of black (top) and green (bottom) traces. Scale bar is 20 μm.

Finally, to show the reversibility of the assembly under changing external stimuli, immobilized GUVs containing NADH, ADH and tdTomato in pH 4.8 buffer were exposed to acetone (20 mM), which rapidly triggered tdTomato membrane assembly (Figure 4, blue arrow). After allowing the assembly process to level off and the lumen/membrane fluorescence intensity ratio to stabilize, disassembly was induced by the substitution of the acetone solution by an *i*PrOH solution (20 mM, Figure 4 yellow arrow). The disassembly process was considerably slower, compared to assembly, yet this was also expected as a result of the ensemble and GUV-based pH measurements (Figure 2 and Figure S3), where the pH decrease also proceeded considerably slower compared to the pH increase. After disassembly had been reached, the cycle was started again to show the full reversibility of the system. Similar time frames were observed for assembly and disassembly in all the imaged GUVs and also in the consecutive cycles.

In conclusion, due to the semi-permeable nature of lipid membranes, an enzymatically induced positional assembly process of proteins in GUVs can be started and controlled using small molecules as external stimuli. In this fashion, we showed that ADH was capable of converting its cofactor upon addition of the small-molecule substrate, thereby directly influencing the internal vesicle pH. As a result, addition of the enzyme substrates also caused a pH gradient to be established over the GUV membranes that could be applied to reversibly induce or inhibit binding of a His_6-tagged fluorescent protein, tdTomato, to Ni-NTA ligands positioned on the GUV membrane. Both Ni-NTA ligand density on the membrane, and the regime in which the pH changes were carried out, proved to be critical parameters for the successful reversible assembly of the protein on the membrane. When operated within the right regime, the system can be cycled between an assembled and disassembled state several times, showcasing the reversible and dynamic nature of this system. Interestingly, as becomes apparent from the traces of individual GUVs presented here, the vesicles each behave slightly different from each other, likely as a result of the formation and content encapsulation mechanism and intrinsic molecular stochastic effects arising from this.

Taken together, these results show that GUVs can be produced that mimic the ability of cells to react to external stimuli by starting a signaling event to induce a reversible structural change inside the vesicle. As NAD^+ and NADH are important cofactors in many biological processes, these simple external stimuli could therefore be used to modulate a host of more complex biological interactions and processes that are linked to these cofactors. Furthermore, also other processes, such as protein-mediated endocytosis and enzyme activity,[19] can be switched on or off using the pH change inside giant vesicles.

Experimental Section

Vesicles were produced as described in the Supporting Information, where 1 mol% of Chol was replaced with 1 mol% of DSPE-PEG2000-biotin. Microscopy slides were functionalized with BSA-biotin (150 μL, 1 mg mL^{-1} in MilliQ) for 2 h and subsequently washed twice with MilliQ to remove unbound protein. The wells were then incubated with streptavidin (150 μL, 0.1 mg mL^{-1} in MilliQ) for 15 min and washed again with MilliQ (2 times) before adding external solution as described above for confocal microscopy experiments. The GUVs were allowed to settle and bind on the surface for 30 min before starting the experiments. Time-lapse imaging was started and the external solution was then substituted with acetone solution at a flow rate of 10 mL h^{-1} for 5 min using syringe pumps (Screening Devices, Amersfoort, The Netherlands), after which the flow was stopped. After protein assembly was achieved, acetone solution was substituted with *i*PrOH solution to trigger assembly, again using a 10 mL h^{-1} flow rate for 5 min. This process was reversed again by changing back to acetone as described before.

Keywords: cell mimic · liposomes · protein–ligand interactions · vesicles

How to cite: *Angew. Chem. Int. Ed.* **2015**, *54*, 9614–9617
Angew. Chem. **2015**, *127*, 9750–9753

[1] a) J. W. Szostak, D. P. Bartel, P. L. Luisi, *Nature* **2001**, *409*, 387–390; b) W. Martin, *Philos. Trans. R. Soc. London Ser. B* **2010**, *365*, 847–855.
[2] a) C. M. Agapakis, P. M. Boyle, P. A. Silver, *Nat. Chem. Biol.* **2012**, *8*, 527–535; b) J. E. Dueber, G. C. Wu, G. R. Malmirchegini, T. S. Moon, C. J. Petzold, A. V. Ullal, K. L. J. Prather, J. D. Keasling, *Nat. Biotechnol.* **2009**, *27*, 753–759.
[3] T. Pawson, P. Nash, *Science* **2003**, *300*, 445–452.
[4] a) C. Martino, S.-H. Kim, L. Horsfall, A. Abbaspourrad, S. J. Rosser, J. Cooper, D. A. Weitz, *Angew. Chem. Int. Ed.* **2012**, *51*, 6416–6420; *Angew. Chem.* **2012**, *124*, 6522–6526; b) V. Noireaux, A. Libchaber, *Proc. Natl. Acad. Sci. USA* **2004**, *101*, 17669–17674; c) G. Murtas, Y. Kuruma, P. Bianchini, A. Diaspro, P. L. Luisi, *Biochem. Biophys. Res. Commun.* **2007**, *363*, 12–17.
[5] a) A. M. Brizard, J. H. Van Esch, *Soft Matter* **2009**, *5*, 1320–1327; b) A. P. Liu, D. A. Fletcher, *Nat. Rev. Mol. Cell Biol.* **2009**, *10*, 644–650; c) R. K. Kumar, M. Li, S. N. Olof, A. J. Patil, S. Mann, *Small* **2013**, *9*, 357–362; d) Y. T. Maeda, T. Nakadai, J. Shin, K. Uryu, V. Noireaux, A. Libchaber, *ACS Synth. Biol.* **2012**, *2*, 53–59; e) E. J. Cabré, A. Sánchez-Gorostiaga, P. Carrara, N. Ropero, M. Casanova, P. Palacios, P. Stano, M. Jiménez, G. Rivas, M. Vicente, *J. Biol. Chem.* **2013**, *288*, 26625–26634.
[6] a) R. J. R. W. Peters, M. Marguet, S. Marais, M. W. Fraaije, J. C. M. van Hest, S. Lecommandoux, *Angew. Chem. Int. Ed.* **2014**, *53*, 146–150; *Angew. Chem.* **2014**, *126*, 150–154; b) L. Hosta-Rigau, O. Shimoni, B. Städler, F. Caruso, *Small* **2013**, *9*, 3573–3583.
[7] X. Huang, M. Li, D. C. Green, D. S. Williams, A. J. Patil, S. Mann, *Nat. Commun.* **2013**, *4*, 2239.
[8] a) M. Marguet, O. Sandre, S. Lecommandoux, *Langmuir* **2012**, *28*, 2035–2043; b) E. Sokolova, E. Spruijt, M. M. K. Hansen, E. Dubuc, J. Groen, V. Chokkalingam, A. Piruska, H. A. Heus, W. T. S. Huck, *Proc. Natl. Acad. Sci. USA* **2013**, *110*, 11692–11697; c) T.-Y. Dora Tang, C. Rohaida Che Hak, A. J. Thompson, M. K. Kuimova, D. S. Williams, A. W. Perriman, S. Mann, *Nat. Chem.* **2014**, *6*, 527–533.
[9] K. Simons, D. Toomre, *Nat. Rev. Mol. Cell Biol.* **2000**, *1*, 31–39.
[10] M. P. Strathmann, N. Gautam, *Science* **1991**, *252*, 802–808.
[11] S. D. Conner, S. L. Schmid, *Nature* **2003**, *422*, 37–44.
[12] A.-L. Barabási, Z. N. Oltvai, *Nat. Rev. Genet.* **2004**, *5*, 101–113.
[13] Y. Huang, Y. Lin, X. Ran, J. Ren, X. Qu, *Nanoscale* **2014**, *6*, 11328–11335.
[14] N. C. Shaner, R. E. Campbell, P. A. Steinbach, B. N. G. Giepmans, A. E. Palmer, R. Y. Tsien, *Nat. Biotechnol.* **2004**, *22*, 1567–1572.
[15] a) J. Schmitt, H. Hess, H. G. Stunnenberg, *Mol. Biol. Rep.* **1993**, *18*, 223–230; b) S. Lata, A. Reichel, R. Brock, R. Tampe, J. Piehler, *J. Am. Chem. Soc.* **2005**, *127*, 10205–10215.
[16] J. D. Patel, R. O'Carra, J. Jones, J. G. Woodward, R. J. Mumper, *Pharm. Res.* **2007**, *24*, 343–352.
[17] a) S. Fujii, T. Matsuura, T. Sunami, T. Nishikawa, Y. Kazuta, T. Yomo, *Nat. Protoc.* **2014**, *9*, 1578–1591; b) S. Pautot, B. J. Frisken, D. A. Weitz, *Langmuir* **2003**, *19*, 2870–2879.
[18] a) D. W. Deamer, R. C. Prince, A. R. Crofts, *Biochim. Biophys. Acta* **1972**, *274*, 323–335; b) P. R. Cullis, M. J. Hope, M. B. Bally, T. D. Madden, L. D. Mayer, D. B. Fenske, *Biochim. Biophys. Acta Rev. Biomembr.* **1997**, *1331*, 187–211; c) D. S. Cafiso, W. L. Hubbell, *Biochemistry* **1978**, *17*, 3871–3877.
[19] S. Kohse, A. Neubauer, A. Pazidis, S. Lochbrunner, U. Kragl, *J. Am. Chem. Soc.* **2013**, *135*, 9407–9411.

Received: March 30, 2015
Published online: June 18, 2015

